Received: 24 February 2022 | Revised: 12 May 2022 | Accepted: 2 June 2022

DOI: 10.1002/psp4.12835

ARTICLE

Longitudinal and time-to-event modeling for prognostic implications of radical surgery in retroperitoneal sarcoma

Ye Yao[1] | **Zhen Wang**[2] | **Ling Yong**[1] | **Qingyu Yao**[1] | **Xiuyun Tian**[2] | **Tianyu Wang**[1] | **Qirui Yang**[1] | **Chunyi Hao**[2] | **Tianyan Zhou**[1]

[1]Beijing Key Laboratory of Molecular Pharmaceutics and New Drug Delivery System, Department of Pharmaceutics, School of Pharmaceutical Sciences, Peking University, Beijing, China

[2]Key Laboratory of Carcinogenesis and Translational Research (Ministry of Education/Beijing), Department of Hepato-Pancreato-Biliary Surgery, Sarcoma Center, Peking University Cancer Hospital and Institute, Beijing, China

Correspondence

Tianyan Zhou, Beijing Key Laboratory of Molecular Pharmaceutics and New Drug Delivery System, Department of Pharmaceutics, School of Pharmaceutical Sciences, Peking University, Beijing 100191, China.
Email: tianyanzhou@bjmu.edu.cn

Chunyi Hao, Key Laboratory of Carcinogenesis and Translational Research (Ministry of Education/Beijing), Department of Hepato-Pancreato-Biliary Surgery, Sarcoma Center, Peking University Cancer Hospital and Institute, Beijing 100142, China.
Email: haochunyi@bjmu.edu.cn

Funding information

Beijing Xisike Clinical Oncology Research Foundation (Approval No. Y-Young 2021-0111), Science Foundation of Peking University Cancer Hospital (Approval No. 2020-14), and Peking University Medicine Seed Fund for Interdisciplinary Research (Approval No. BMU2021MX003)

Abstract

Retroperitoneal sarcoma (RPS) is a rare malignancy which can be difficult to manage due to the variety of clinical behaviors. In this study, we aimed to develop a parametric modeling framework to quantify the relationship between postoperative dynamics of several biomarkers and overall/progression-free survival of RPS. One hundred seventy-four patients with RPS who received surgical resection with curative intent at the Peking University Cancer Hospital Sarcoma Center were retrospectively included. Potential prognostic factors were preliminarily identified. Longitudinal analyses of body mass index (BMI), serum total protein (TP), and white blood cells (WBCs) were performed using nonlinear mixed effects models. The impacts of time-varying and time-invariant predictors on survival were investigated by parametric time-to-event (TTE) models. The majority of patients experienced decline in BMI, recovery of TP, as well as transient elevation in WBC counts after surgery, which significantly correlated with survival. An indirect-response model incorporating surgery effect described the fluctuation in percentage BMI. The recovery of TP was captured by a modified Gompertz model, and a semi-mechanistic model was selected for WBCs. TTE models estimated that the daily cumulative average of predicted BMI and WBC, the seventh-day TP, as well as certain baseline variables, were significant predictors of survival. Model-based simulations were performed to examine the clinical significance of prognostic factors. The current work quantified the individual trajectories of prognostic biomarkers in response to surgery and predicted clinical outcomes, which would constitute an additional strategy for disease monitoring and intervention in postoperative RPS.

Study Highlights

WHAT IS THE CURRENT KNOWLEDGE ON THE TOPIC?

Risk stratification of many cancer types consist of time-varying biochemical or physical biomarkers. Integrative quantitative analytics are necessary to allow for

Ye Yao and Zhen Wang contributed equally to this work.

the identification of similar relationships in retroperitoneal sarcoma (RPS) following radical surgical resection.

WHAT QUESTION DID THIS STUDY ADDRESS?

The postoperative dynamics of multiple prognostic biomarkers, including body mass index (BMI), serum total protein (TP), and white blood cells (WBCs), as well as their predictive values for overall survival (OS) and progression-free survival (PFS) were investigated.

WHAT DOES THIS STUDY ADD TO OUR KNOWLEDGE?

The impact of radical surgery on longitudinal BMI, TP, and WBCs were quantified using pharmacometric approaches for the first time. Early changes in those biomarkers could be informative for OS and PFS of RPS.

HOW MIGHT THIS CHANGE DRUG DISCOVERY, DEVELOPMENT, AND/OR THERAPEUTICS?

This joint modeling framework provides a novel methodology for clinical outcome prediction in surgical oncology leveraging baseline and early biomarker data. Quantitative advice on optimized clinical surveillance and interventions for patients at risk of malnutrition, hypoproteinemia, and leukocytosis can potentially improve quality of life.

INTRODUCTION

Soft tissue sarcoma accounts for less than 1% of adult malignancies, among which 15% are retroperitoneal sarcoma (RPS).[1,2] Radical surgical resection is currently the sole potentially curative method for RPS, and the clinical benefits of other therapeutics are still doubtable.[3,4] However, the asymptomatic features of early-stage disease lead to frequent diagnosis with large tumors, adding to the difficulty in complete resection along with the possibility for relapse.[4–6] Patients often suffer from postoperative complications and impaired quality of life, sometimes impacting clinical outcomes and even survival.[7,8] The 5-year overall survival (OS) of RPS ranges from 39% to 65%,[9] and 41%–70% of patients demonstrate local recurrence.[2]

The existing prognostic analysis of RPS focused on clinicopathologic and treatment characteristics, such as age, tumor grade, histologic subtype, extent of resection, etc., mainly using semiparametric methodologies.[6,10–13] However, recent studies have demonstrated the value of incorporating continuous progression profiles of various biological or physical biomarkers, apart from time-invariant covariates, in oncologic survival analysis, including but not limited to tumor size, therapeutic targets, and disease-specific clinical variables.[14–19] This calls for development of paradigms linking quantitative models describing time-varying biomarkers to models predicting clinical outcomes.[20,21] Longitudinal tumor size following treatment with durvalumab was linked to OS of urothelial carcinoma using a population tumor kinetic model plus a time-to-event (TTE) model.[14] Irurzun-Arana et al. identified dynamic change in lactate dehydrogenase (LDH) as the most significant predictor of OS in melanoma.[17] Such analysis has so far not been reported for RPS.

Pharmacometric approaches have contributed significantly to drug development through quantifying and predicting pharmacokinetics, pharmacodynamics, and disease progression.[22] Nonlinear mixed effects modeling is a standard tool for processing population longitudinal data where high inter- and intra-individual variability, commonly observed in clinic, can be described, and covariate relationships accounting for systematic differences between individuals are evaluated.[23,24] Parametric TTE modeling allows quantification of a time-varying covariate's implication on survival time, along with estimation of baseline hazard.[25,26] These quantitative tools have been seldomly used in surgical oncology where perioperative physical and biological disorders are often observed and may have implications for survival.

In this study, we retrospectively explored an in-house database of Chinese patients with RPS following surgical resection. Leveraging population longitudinal and TTE modeling strategies, we aimed to characterize the postoperative dynamics of key prognostic biomarkers and predict the clinical end points (i.e., OS and progression-free survival [PFS]). This joint modeling approach allowed us to make a quantitative inference from early continuous

biomarker data to predict survival outcomes of RPS for the first time.

METHODS

Study population

Patients with RPS who have received surgical resection with curative intent between 2011 and 2020 at the Peking University Cancer Hospital Sarcoma Center were retrospectively collected. Following the inclusion/exclusion criteria specified in the Supplementary Material, 174 Chinese adult patients with RPS were considered eligible and were finally enrolled in our modeling database. The study was approved by the ethics committee of the Peking University Cancer Hospital. Patients provided written informed consent for data collection.

Data collection and exploratory data analysis

Demographics, clinicopathologic characteristics, and treatment details of the patients were recorded. Continuous data of body mass index (BMI), tumor size, hematology, and chemistry laboratory values, which have been repeatedly measured perioperatively, were collected. OS was defined as the time from surgery to death, and PFS was the time from surgery to tumor relapse or death, whichever occurred first. Exploratory survival analyses were performed using Kaplan–Meier analysis and Cox regression to identify potential prognostic factors. Apart from baseline characteristics, longitudinal data, such as BMI and laboratory values, were converted to cross-sectional variables for analysis, by calculating the average values during periods before or after surgery.

Population longitudinal submodels for postoperative dynamics of biomarkers

The postoperative changes in promising prognostic biomarkers were described using various longitudinal model structures with schematic representations in Figure S1. Briefly, an indirect-response (IDR) model was selected for the turnover of percentage BMI (hereinafter referred to as BMI for simplification) assuming a steady-state tumor-free BMI of 100% for each subject.[27] The stimulatory effect of surgery on the loss of BMI decayed in an exponential manner from its maximum on day 0; conversely, interventions, such as nutrition supply, could accelerate the zero-order input.

The recovery of serum total protein (TP) after surgery was captured by a modified Gompertz model.[28] The postoperative trough and steady-state levels of TP, as well as the recovery rate constant, were estimated. The model also incorporated an additional possible disturbance due to a subsequent invasive operation.

The starting point for describing the longitudinal white blood cell (WBC) observations was the semimechanistic myelosuppression model, which was reversed to characterize the acute increase in WBC counts after surgery.[29,30] The proliferation of progenitor cells was promoted by a time-dependent surgery effect. In addition, tumor resection as well as subsequent invasive operations also triggered the immediate release of WBCs from the deposit pool.

TTE models for survival analysis

Parametric TTE models were developed to investigate the effect of potential predictors on OS and PFS hazards, $h(t)$. The baseline hazard $h_0(t)$ was explored using exponential, Weibull, and log-logistic models.[25] Potential predictors were then added to the following hazard function:

$$h_i\left(t|X_i\right)=h_0(t)\cdot\exp\left(\sum_{j=1}^{p}\gamma^j\left(Z_i^j-\text{median}\left(Z^j\right)\right)+\sum_{j=p+1}^{p+q}\gamma^j Z_i^j\right)\cdot\exp\left(\sum_{j=1}^{r}\beta^j f^j\left(t,X_i\right)\right) \quad (1)$$

where Z_i and X_i depict constant and time-varying predictors in i^{th} subject, respectively. γ^j and β^j are coefficients associated with the effect of j^{th} predictor. $f\left(t, X_i\right)$ is a link function. p, q, r are the total number of continuous constant predictors, discrete constant predictors, and time-varying predictors, respectively. Constant predictors tested on OS and/or PFS included tumor grade defined by the French Federation of Cancer Centers Sarcoma Group (FNCLCC),[1] baseline metastasis, resected tumor volume, completeness of resection, fibrinogen, and postoperative tumor relapse.

A sequential modeling strategy was adopted to explore the correlations among time-varying BMI, TP, WBCs, and survival. Individual empirical Bayes estimates (EBEs) from the longitudinal submodels were used to predict time-courses of the biomarkers, as well as model-derived metrics, which were then investigated as predictors in the TTE models.[15] Prognostic baseline variables were also screened and added to the proportional hazard functions.

Model construction and evaluation

Nonlinear mixed effects models were developed using NONMEM 7.4.1 and PsN 4.9.0 managed by Pirana 2.9.9,

with first-order conditional estimation with interaction and Laplace method for longitudinal and TTE models, respectively. A stepwise forward selection followed by backward elimination procedure was performed during covariate evaluation. An objective function value (OFV) decrease of 3.84 ($X^2_{\alpha=0.05,\nu=1}$) was considered as statistically significant during forward selection of a covariate, and an increase of 10.83 ($X^2_{\alpha=0.001,\nu=1}$) during backward elimination (6.64 based on $X^2_{\alpha=0.01,\nu=1}$ for TTE models). Interindividual variability of model parameters was assumed to be log-normally distributed and expressed as coefficient of variation (CV), and an additive, proportional, or additive plus proportional error model was selected to describe the residual variability. Parameter uncertainties were derived from 1000-time bootstrapping or the NONMEM Sandwich matrix.[31] Evaluation of model performance depended on the rationality and precision (expressed as relative standard error [RSE]) of the parameter estimates, decline in OFV, diagnostic plots, and visual predictive check (VPC) outcomes. Bootstrap and Sampling Importance Resampling were also performed for model validation. Example model code and datasets are provided in Supplementary Material, and the original data are available upon request.

Model simulation

The impacts of critical variables on OS and PFS were visualized through joint model-based simulations of 500 virtual cohorts with 500 subjects in each cohort randomly resampled from the modeling dataset. The individual time-varying predictors were simulated based on population longitudinal submodels, followed by TTE model-based simulations of survival, incorporating parameter uncertainty, interindividual variability, and current distribution of patient baseline characteristics. Kaplan–Meier curves were compared between subgroups of each covariate.

RESULTS

Identification of time-varying prognostic factors

The patient characteristics are summarized in Table 1. Patients were followed up with a median period of 18.4 months. The median OS and PFS were 43.6 months and 15.8 months, respectively.

Exploratory data analysis showed that the majority of patients in our database experienced loss of BMI, abnormally low serum TP, as well as elevated WBCs after surgery. As illustrated by the Kaplan–Meier curves in Figure 1, these variables significantly correlated with OS and PFS. Therefore, population longitudinal submodels were developed to investigate the dynamics of the three promising biomarkers.

TABLE 1 Demographic, clinicopathologic, and treatment characteristics of patients

Variable	Median [range]/ strata	*n* (%)
Age, years	57 [18, 81]	174 (100)
Gender	Female	87 (50.0)
	Male	87 (50.0)
Ethnic group	Han	164 (94.3)
	Other	10 (5.7)
ECOG	Grade 0	156 (89.7)
	Grade 1 and higher	18 (10.3)
Histologic subtype	Liposarcoma	115 (66.1)
	Leiomyosarcoma	29 (16.7)
	Other	30 (17.2)
FNCLCC grade	1	25 (14.4)
	2	66 (37.9)
	3	83 (47.7)
Baseline metastasis	Yes	39 (22.4)
	No	135 (77.6)
Multifocality	Yes	55 (31.6)
	No	119 (68.4)
Presentation status	Primary	99 (56.9)
	Recurrent	75 (43.1)
Resected tumor volume, cm^3	1172.38 [2.4, 18,000]	174 (100)
Resected organs	6 [0, 14]	174 (100)
Surgical blood loss, ml	1000 [50, 16,000]	174 (100)
Completeness of resection	Yes	142 (81.6)
	No	32 (18.4)
Fibrinogen, mg/dL	436.1 [175.7, 1176.0]	171 (98.3)
Baseline BMI, kg/m^2	23.2 [15.7, 39.0]	174 (100)
Baseline TP, g/L	62.6 [48.0, 80.2]	173 (99.4)
Baseline WBCs, 10^9cells/L	6.20 [2.87, 35.67]	174 (100)
Subsequent invasive operation time, day	114 [18, 330]	64 (36.8)

Abbreviations: BMI, body mass index; ECOG, Eastern Cooperative Oncology Group; FNCLCC, French Federation of Cancer Centers Sarcoma Group; TP, total protein; WBCs, white blood cells.

BMI submodel

The dynamics of BMI following surgical resection was characterized using an IDR model with bidirectional actions (Figure S1A). The stimulatory effect of surgery on

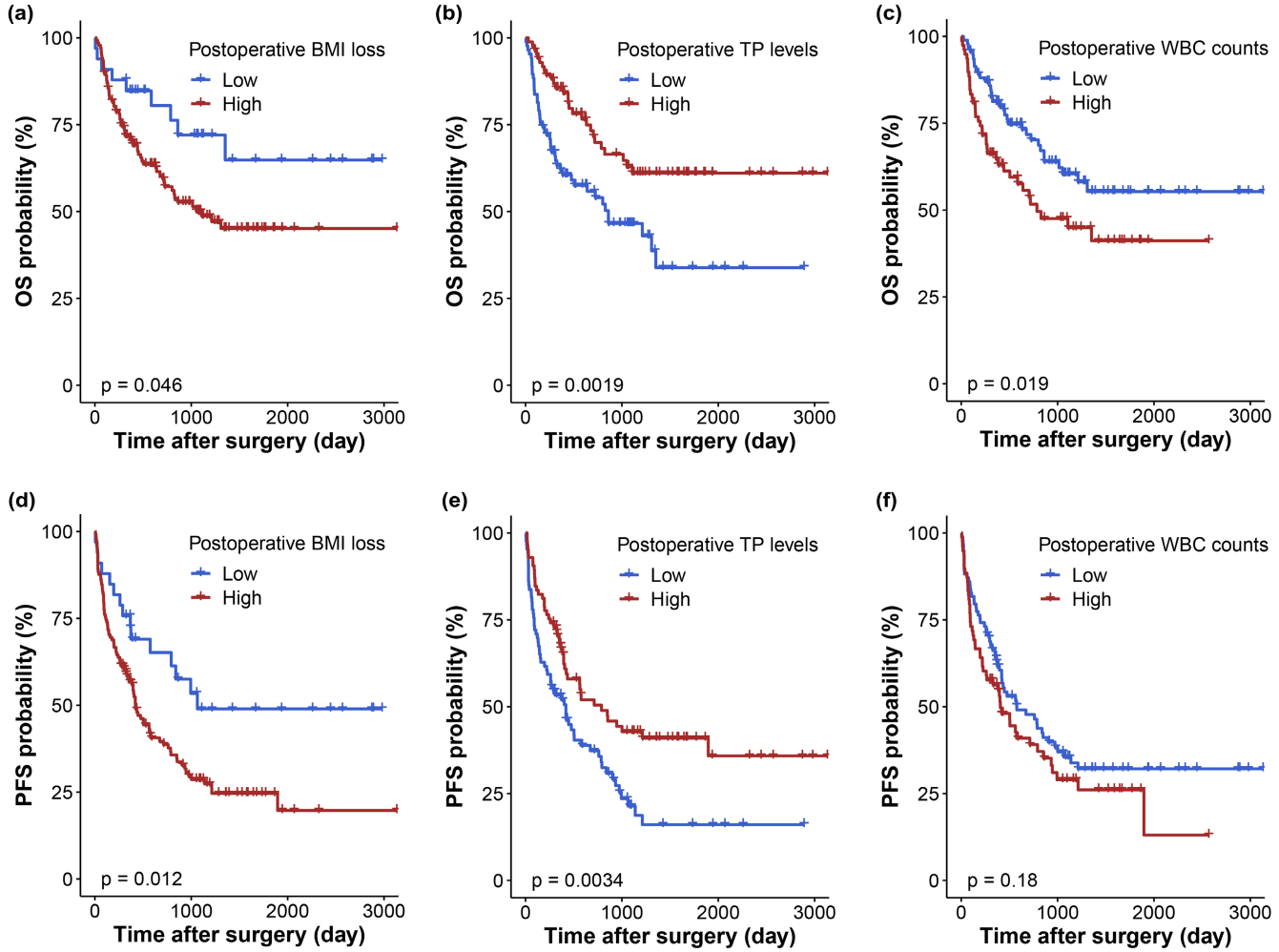

FIGURE 1 Kaplan–Meier curves of OS and PFS stratified by postoperative BMI loss (a, d), TP levels (b, e), and WBC counts (c, f). The cutoff values were 0.6 kg/m^2 for BMI loss, 55.7 g/L for TP, and 10.72×10^9 cells/L for WBCs. Log-rank test was performed and *p* value was shown in each panel. BMI, body mass index; OS, overall survival; PFS, progression-free survival; TP, total protein; WBC, white blood cell.

the loss of BMI (K_{OUT}) decayed in an exponential manner with a rate constant of λ_1 from its maximum, SUR_{MAX}, on day 0. Conversely, there were interventions, such as parenteral nutrition supply accelerating K_{IN}, which were quantified similarly by STI_{MAX} and λ_2.

$$\frac{dBMI}{dt} = K_{IN} \cdot \left(1 + STI_{MAX} \cdot e^{-\lambda_2 \cdot t}\right) - K_{OUT} \cdot \left(1 + SUR_{MAX} \cdot e^{-\lambda_1 \cdot t}\right) \cdot BMI, \quad BMI(t=0) = BMI_0 \tag{2}$$

$$K_{IN} = K_{OUT} \cdot 100 \tag{3}$$

Parameter estimates of the final BMI submodels were reported in Table 2. The typical value of baseline BMI (BMI_0) was 97.5% right before surgery, indicating a minor decline in body weight since the onset of cancer. Competition between stimulatory effects on K_{IN} and K_{OUT} resulted in varied patterns of BMI change in the population. A long half-life of 109 days was estimated for surgery effect, depicting a durable impairment in patients' physical status. Following evaluation of a number of covariates among demographic, clinicopathologic, and treatment variables, resected tumor volume significantly correlated with BMI turnover rate (K_{IN}), and a higher number of resected organs resulted in slower decay rate constant of surgery effect. Patients with a lower tumor-free BMI exhibited larger K_{IN}-stimulating effect in our cohort. The functions describing covariate effects in the longitudinal submodels as well as their clinical relevance can be found in the Supplementary Material. The VPC result in Figure 2a demonstrated good agreement between observed and simulated BMI data.

TP submodel

A modified Gompertz model well captured the time-courses of TP (Figure S1B). TP increased from the postoperative trough level (TP_{POST}) to a steady-state (TP_{SS}) with

TABLE 2 Parameter estimates of the final longitudinal submodels

Parameter	Definition	Estimate (RSE%[a])	IIV, CV% (RSE%[a])
BMI submodel			
K_{IN}(%/day)	Production rate constant	0.971 (19.5)	74.4 (16.8) [34][b]
θ_{RESTV}	Resected tumor volume on K_{IN}	0.358 (19.6)	–
BMI_0(%)	Baseline BMI	97.5 (0.5)	5.4 (12.7) [6]
SUR_{MAX}	Maximum surgery effect	0.834 (9.8)	0 FIX
λ_1/day	Decay rate constant of surgery effect	0.00634 (19.5)	72.9 (23.8) [40]
θ_{RESOR}	Resected organ number on λ_1	−0.119 (30.2)	–
STI_{MAX}	Maximum K_{IN}-stimulating effect	0.338 (17.9)	32.0 (38.3) [55]
$\theta_{BMI_{tumor-free}}$	Tumor-free BMI on STI_{MAX}	−1.93 (45.0)	–
λ_2/day	Decay rate constant of K_{IN}-stimulating effect	0.00512 (37.0)	0 FIX
σ_{add}(%)	Additive error	2.50 (5.0) [20]	–
TP submodel			
K_{PRO}/day	Production rate constant	0.0859 (10.2)	79.2 (10.1) [23]
TP_{POST}, g/L	Postoperative instant TP	48.3 (1.1)	9.2 (8.3) [17]
θ_{BLLO}	Surgical blood loss on TP_{POST}	−0.00414 (12.2)	–
θ_{MULTI}	Multifocality on TP_{POST}	−0.0743 (22.6)	–
TP_{SS}, g/L	Steady-state TP	67.9 (1.1)	7.3 (11.5) [30]
DIS_{MAX}/day	Maximum subsequent disturbance	0.0576 (19.7)	161.1 (12.9) [45]
λ/day	Decay rate constant of subsequent disturbance	0.336 (18.4)	0 FIX
σ_{prop}(%)	Proportional error	8.84 (3.5) [10]	–
WBC submodel			
MTT, day	Mean transit time	4.91 (0.7)	21.4 (13.5) [35]
$CIRC_0$, 10^9 cells/L	Baseline WBC count	6.25 (0.8)	32.8 (13.0) [15]
θ_{LNFIB}	Logarithm of fibrinogen on $CIRC_0$	1.78 (14.4)	–
$CIRC_{SS}$, 10^9 cells/L	Steady-state WBC count	6.92 (1.3)	32.0 (10.8) [20]
$\theta_{RESOR\_CIRC_{SS}}$	Resected organ number on $CIRC_{SS}$	0.0362 (14.1)	–
γ	Feedback loop factor on proliferation rate	0.119 (9.2)	70.3 (14.4) [30]
SUR_{MAX}	Maximum surgery effect	0.798 (1.6)	0 FIX
$\theta_{RESOR\_SUR_{MAX}}$	Resected organ number on SUR_{MAX}	0.315 (10.5)	–
λ/day	Decay rate constant of surgery effect	0.453 (3.5)	23.9 (20.4) [47]
$DEPOS_0$, 10^9cells/L	Initial WBC count in the deposit pool	15.1 (1.0)	62.4 (13.3) [26]
K_{RELE}/day	Release rate constant from the deposit pool	0.423 (3.4)	0 FIX
σ_{prop}(%)	Proportional error	25.6 (5.0) [10]	–
σ_{add}, 10^9 cells/L	Additive error	0.919 (22.0) [10]	–

Abbreviations: BMI, percentage body mass index; CV, coefficient of variation; IIV, interindividual variability; MTT, mean transit time; RSE, relative standard error; TP, total protein; WBC, white blood cell.

[a]Obtained from bootstrap results.

[b]η- and ε-shrinkage (%) in square brackets.

a first-order rate, K_{PRO}, until an additional possible disturbance occurred due to another invasive operation (stoma closure, exploratory laparotomy, etc.) at t_{DIS}. The disturbance effect was assumed to decay in an exponential manner with a rate constant of λ from its maximum (DIS_{MAX}) at t_{DIS}.

$$\frac{dTP}{dt} = K_{PRO} \cdot TP \cdot LOG\left(\frac{TP_{SS}}{TP}\right) - DIS \cdot TP, TP(t=0) = TP_{POST} \quad (4)$$

$$DIS = \begin{cases} 0, t < t_{DIS} \\ DIS_{MAX} \cdot e^{-\lambda \cdot (t - t_{DIS})}, t \geq t_{DIS} \end{cases} \quad (5)$$

An estimated TP_{POST} of 48.3 g/L was consistent with the commonly observed TP levels falling below the lower limit of reference range right after surgery, and it was even lower for subjects with more surgical blood loss or tumor

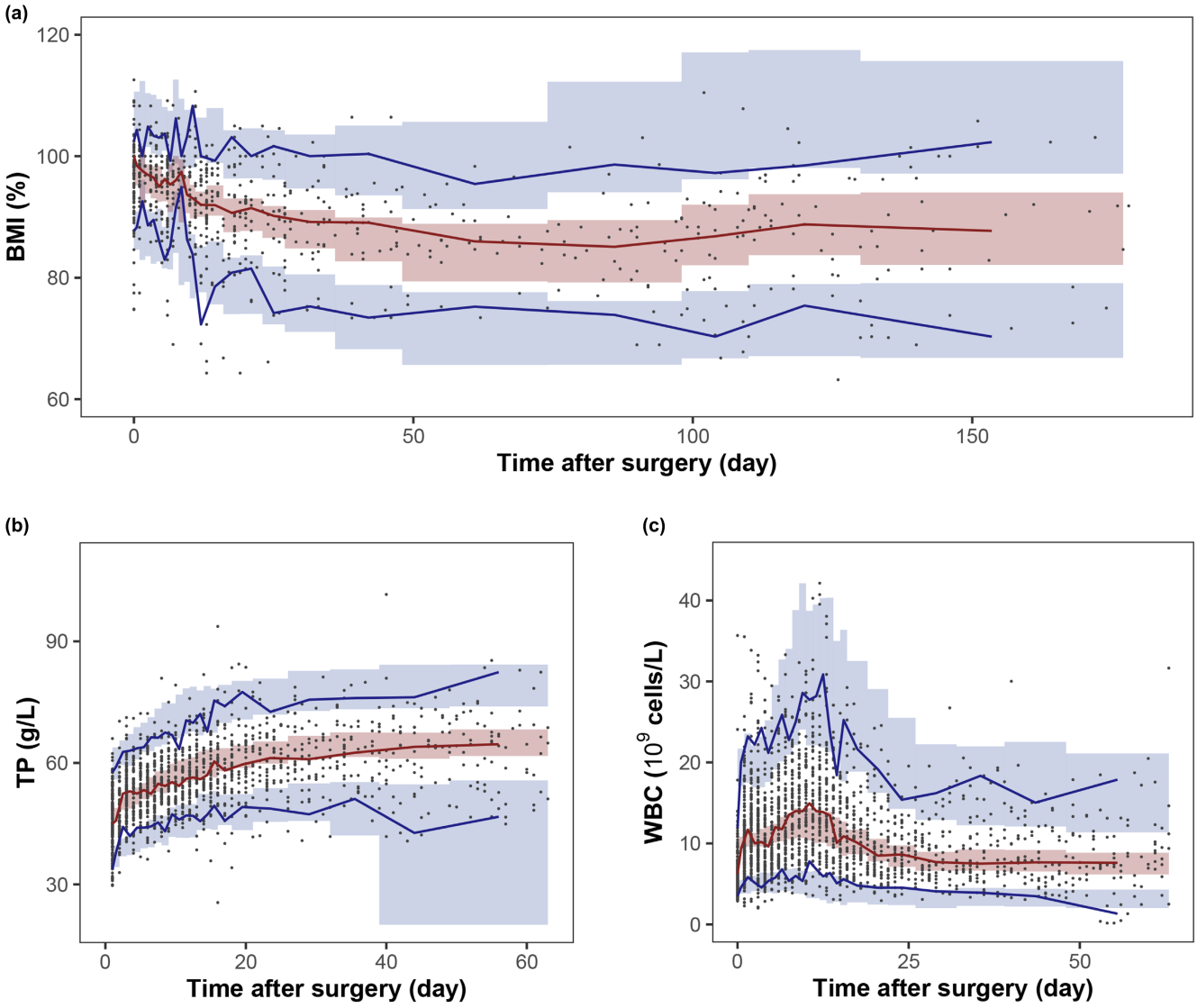

FIGURE 2 Visual predictive check for the longitudinal submodels of BMI (a), TP (b), and WBC (c). The dots represent the observed individual data. The red line in each panel represents the observed median, and blue lines represent the observed 5th and 95th percentiles. Shaded areas show 95% confidence intervals of model-predicted median (red), 5th and 95th percentiles (blue) based on 1000-time simulations. Plots are presented on partial time scales and the entire illustrations could be found in Figure S2. BMI, percentage body mass index; TP, total protein; WBC, white blood cell.

multifocality. High interindividual variability with CV of 161.1% was found in DIS_{MAX} describing the subsequent disturbance due to a small proportion (36.8%) in this subpopulation. The model demonstrated acceptable predictive performance both on a shorter and longer time scale (Figures 2b and S2B).

WBC submodel

The semimechanistic WBC model shown in Figure S1C consisted of one compartment that represented proliferative cells (*PROL*), three transit compartments with maturing cells (*TRANS1, 2,* and *3*), a compartment of circulating observed WBC (*CIRC*), and a deposit pool in bone marrow (*DEPOS*). A rapid increase in circulating WBC counts was driven by the immediate release from the deposit pool, followed by a profound and sustained response to surgery through the transit chain. The equations of the WBC submodel are as follows:

$$\frac{\mathrm{dPROL}}{\mathrm{d}t} = K_{\mathrm{PRO}} \cdot \left(1 + \mathrm{SUR}_{\mathrm{MAX}} \cdot \mathrm{e}^{-\lambda \cdot t}\right) \cdot \mathrm{PROL} \cdot \left(\frac{\mathrm{CIRC}_{\mathrm{ss}}}{\mathrm{CIRC}}\right)^{\gamma} - K_{\mathrm{TR}} \cdot \mathrm{PROL} \quad (6)$$

$$\frac{\mathrm{dTRANS1}}{\mathrm{d}t} = K_{\mathrm{TR}} \cdot (\mathrm{PROL} - \mathrm{TRANS1}) \quad (7)$$

$$\frac{\mathrm{dTRANS2}}{\mathrm{d}t} = K_{\mathrm{TR}} \cdot (\mathrm{TRANS1} - \mathrm{TRANS2}) \tag{8}$$

$$\frac{\mathrm{dTRANS3}}{\mathrm{d}t} = K_{\mathrm{TR}} \cdot (\mathrm{TRANS2} - \mathrm{TRANS3}) \tag{9}$$

$$\begin{aligned}\frac{\mathrm{dCIRC}}{\mathrm{d}t} &= K_{\mathrm{TR}} \cdot \mathrm{TRANS3} - K_{\mathrm{OUT}} \cdot \mathrm{CIRC} \\ &+ \mathrm{DEPOS} \cdot K_{\mathrm{RELE}}, \mathrm{CIRC}(t=0) = \mathrm{CIRC}_0\end{aligned} \tag{10}$$

$$\begin{aligned}\frac{\mathrm{dDEPOS}}{\mathrm{d}t} &= -\mathrm{DEPOS} \cdot K_{\mathrm{RELE}}, \mathrm{DEPOS}(t=0) \\ &= \mathrm{DEPOS}\left(t = t_{\mathrm{DIS}}\right) = \mathrm{DEPOS}_0\end{aligned} \tag{11}$$

$$K_{\mathrm{PRO}} = K_{\mathrm{TR}} = K_{\mathrm{OUT}} = \frac{4}{\mathrm{MTT}} \tag{12}$$

The proliferation of progenitor cells (K_{PRO}) accelerated after surgery, whose effect decayed in an exponential manner from its maximum, $\mathrm{SUR}_{\mathrm{MAX}}$, on day 0. Radical surgical resection as well as subsequent invasive operations at t_{DIS} also triggered the immediate release of WBCs from the deposit pool at a first-order rate constant, K_{RELE}. The other parameters were defined as in the original literature.[29] The preoperative baseline WBC count (CIRC_0) was 6.25×10^9 cells/L, and the steady-state ($\mathrm{CIRC}_{\mathrm{SS}}$) was 6.92×10^9 cells/L in this dataset. The half-life of surgery effect stimulating cell proliferation was estimated to be 1.53 days. Significant covariates included resected organ number and baseline fibrinogen. The model was adequate to capture the WBC profiles within 8 weeks (Figure 2c). The majority of parameter estimates from the three submodels were reasonable with acceptable precision. Goodness-of-fit plots are shown in Figure S3.

TTE models of OS and PFS

The baseline hazards of OS and PFS were both best described using exponential models. Postoperative BMI, TP, and WBCs were incorporated into the final parametric TTE models. Individual time-courses were predicted using EBEs from the above submodels (see Figure S4), and the following link functions were finally selected for time-varying predictors:

$$f(t, \mathrm{BMI}) = \mathrm{BMI}_{\mathrm{AVE}}(t) - 100 \tag{13}$$

$$f(t, \mathrm{TP}) = \min\left(\mathrm{TP}_{\mathrm{DAY7}} - 60, 0\right) \tag{14}$$

$$f(t, \mathrm{WBC}) = \begin{cases} \max\left(\mathrm{WBC}_{\mathrm{AVE}}(t) - 10, 0\right), t \le 56 \\ \max\left(\mathrm{WBC}_{\mathrm{AVE}}(t=56) - 10, 0\right), t > 56 \end{cases} \tag{15}$$

where $\mathrm{BMI}_{\mathrm{AVE}}(t)$is the cumulative average of BMI predictions from day 0 to day t. Similarly, $\mathrm{WBC}_{\mathrm{AVE}}(t)$ is the cumulative average of WBC predictions from day 0 to day t. $\mathrm{TP}_{\mathrm{DAY7}}$ is the predicted TP level on day 7. Hazard functions of the final TTE models are shown in Equations 16 and 17, and parameter estimates are listed in Table 3.

$$\begin{aligned}h_{\mathrm{OS}}(t) &= \lambda_{0,\mathrm{OS}} \cdot \exp\left(\gamma_{\mathrm{META}} \cdot \mathrm{META} + \gamma_{\mathrm{LNFIB}} \cdot (\mathrm{LNFIB} - 6.06)\right) \\ &\cdot \exp\left(\beta_{\mathrm{BMI}} \cdot f(t, \mathrm{BMI}) + \beta_{\mathrm{TP}} \cdot f(t, \mathrm{TP}) + \beta_{\mathrm{WBC}} \cdot f(t, \mathrm{WBC})\right)\end{aligned} \tag{16}$$

$$\begin{aligned}h_{\mathrm{PFS}}(t) &= \lambda_{0,\mathrm{PFS}} \cdot \exp\left(\gamma_{\mathrm{META}} \cdot \mathrm{META} + \gamma_{\mathrm{COMP}} \cdot \mathrm{COMP}\right. \\ &\left. + \gamma_{\mathrm{GRADE}} \cdot \mathrm{GRADE}\right) \cdot \exp\left(\beta_{\mathrm{TP}} \cdot f(t, \mathrm{TP}) + \beta_{\mathrm{WBC}} \cdot f(t, \mathrm{WBC})\right)\end{aligned} \tag{17}$$

where $\lambda_{0,\mathrm{OS}}$ and $\lambda_{0,\mathrm{PFS}}$ are constant baseline hazards of death and disease progression, respectively. META, COMP, and GRADE are dichotomous variables indicating the presence of baseline metastasis, incomplete resection, and FNCLCC grade 3, respectively. LNFIB is a logarithm of baseline fibrinogen. The other parameters have been defined before. The magnitude of baseline hazards was quite small in line with the observed event times. An increase in TP or BMI was beneficial for survival, whereas higher WBC counts raised the hazards of death and disease progression. None of the 95% confidence intervals for the model parameters reported included the value of zero, indicating that the data supported the inclusion of the above predictors in the final models. The predictive performance was acceptable (Figure 3).

Model-based simulation and risk stratification

In order to further explore the impacts of various covariates from the longitudinal submodels and TTE models on OS and PFS, joint model-based simulations were performed in 500 virtual cohorts. As shown in Figure 4, stratifications by baseline metastasis, fibrinogen (predictors identified in the TTE models), tumor-free BMI, resected tumor volume (covariates affecting BMI), surgical blood loss, or multifocality (covariates affecting TP) categorized patients into subgroups at higher or lower risk. Clinical outcomes could also be distinguished based on differences in 12-month BMI, seventh-day TP, and 8-week WBCs. Lower OS probability was predicted for patients with BMI loss over 5% on average, or abnormality in TP or WBCs. PFS simulations are presented in Figure S5.

TABLE 3 Parameter estimates of the final TTE models

Parameter	Definition	Estimate (RSE%[a])	SIR median (95% CI)
OS model			
$\lambda_0(10^{-4}/day)$	Constant baseline hazard	1.22 (24.0)	1.28 (0.76, 1.88)
β_{BMI}	Coefficient associated to BMI	−0.0565 (23.0)	−0.0552 (−0.0288, −0.0830)
β_{TP}	Coefficient associated to TP	−0.131 (19.2)	−0.127 (−0.081, −0.173)
β_{WBC}	Coefficient associated to WBC	0.213 (35.7)	0.215 (0.061, 0.351)
γ_{META}	Coefficient associated to baseline metastasis	1.16 (21.0)	1.15 (0.66, 1.59)
γ_{LNFIB}	Coefficient associated to logarithm of fibrinogen	1.36 (22.4)	1.35 (0.77, 1.92)
PFS model			
$\lambda_0(10^{-4}/day)$	Constant baseline hazard	3.21 (20.9)	3.28 (2.18, 4.57)
β_{TP}	Coefficient associated to TP	−0.105 (22.9)	−0.103 (−0.064, −0.140)
β_{WBC}	Coefficient associated to WBC	0.256 (26.7)	0.256 (0.128, 0.376)
γ_{META}	Coefficient associated to baseline metastasis	1.05 (27.4)	1.04 (0.57, 1.45)
γ_{COMP}	Coefficient associated to incomplete resection	1.12 (27.3)	1.12 (0.63, 1.59)
γ_{GRADE}	Coefficient associated to FNCLCC grade 3	0.698 (30.1)	0.678 (0.297, 1.06)

Abbreviations: BMI, percentage body mass index; CI, confidence interval; FNCLCC, French Federation of Cancer Centers Sarcoma Group; OS, overall survival; RSE, relative standard error; SIR, Sampling Importance Resampling; TP, total protein; TTE, time-to-event; WBC, white blood cell.

[a]Obtained from NONMEM Sandwich matrix.

DISCUSSION

The individual patient survival after RPS surgery can vary tremendously and is a function of multiple influencing factors, including disease-specific baseline characteristics and postoperative complications, such as malnutrition, cachexia, and infection.[9,11] This work characterized the dynamics of key prognostic biomarkers following radical surgical resection in patients with RPS by population longitudinal modeling, and established quantitative models to predict postoperative prognosis of patients with RPS based on time-varying covariates for the first time. The joint model outperformed the existing nomograms commonly used in the clinic, which are based on merely baseline variables. The current results provided useful insights to identify patient subgroups at higher risk and guide optimal clinical interventions regarding the significant predictors.

Laboratory values from hematology and chemistry tests as well as body weight are standardized biomarkers routinely monitored in clinic, and their prognostic significance as static metrics have been reported in oncology.[32,33] Weight loss in patients with gastric and pancreatic cancer has implications for survival.[34,35] Patients with higher inflammatory markers, such as WBC, on the third day after surgery, or those with malnutrition indicated by lower serum albumin or TP, had impaired survival.[36–39] However, those variables are continuously fluctuating in patients with cancer, especially following invasive operations, so investigation on the dynamic relationships allows more meaningful predictions of prognosis. In contrast to previous studies, our modeling framework utilized the entire longitudinal profiles of key biomarkers, rather than cross-sectional data, thus enabling a more accurate assessment of the quantitative relationship between each biomarker

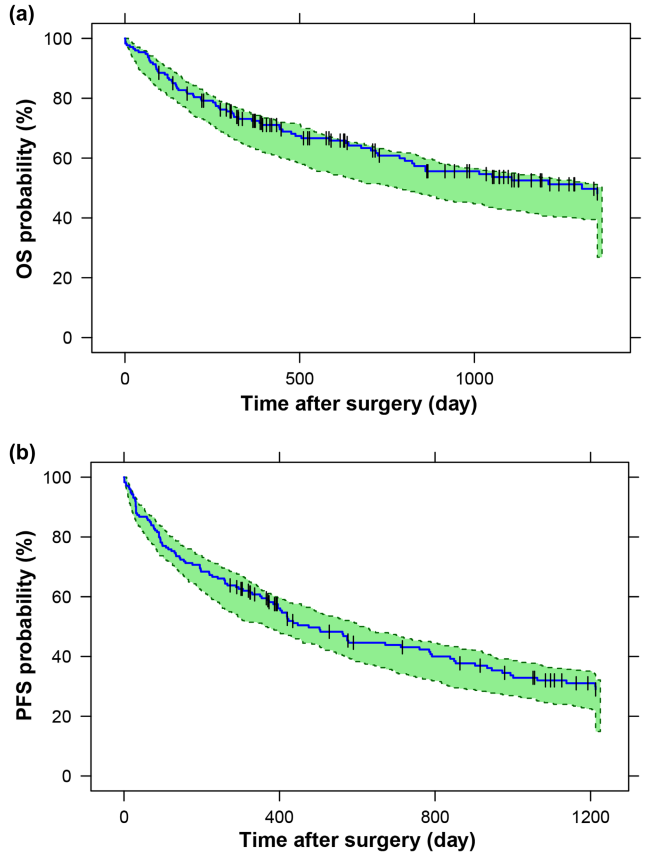

FIGURE 3 Visual predictive check for the TTE models of OS (a) and PFS (b). The solid line in each panel represents the observed Kaplan–Meier curve. The shaded area shows 95% confidence interval of model-predicted Kaplan–Meier curve based on 100-time simulations. OS, overall survival; PFS, progression-free survival; TTE, time-to-event.

and survival.[17] Accordingly, personalized prediction of survival probabilities for different scenarios could be performed using the established parametric TTE models. Besides, a nonlinear mixed effects modeling strategy enabled model-based extrapolation of missing longitudinal data so that bias resulted from opportunistic sampling in the clinic can be reduced during survival analysis.[24]

The longitudinal model structures were finalized after a lot of attempts of model selection and modification. An IDR model well quantified a delayed response to surgery for BMI in contrast with the rapid changes observed in TP and WBCs. Surgery effect was quantified as in a kinetic/pharmacodynamic model.[40] The generally monotonic TP trajectories before additional disturbance supported model construction based on merely postoperative data for simplification. The high magnitude of interindividual variability in DIS_{MAX} mainly resulted from the varied type of subsequent invasive operations and limited subgroup size. The semimechanistic WBC model estimated normal preoperative and steady-state levels, but intermediate fluctuation to distinct extents for different subjects, with physiological parameters consistent with reported values.[41] The covariate relationships were in line with our clinical experience and other researches in surgical oncology. The population longitudinal submodels described multiple levels of variability and demonstrated adequate predictive performance within the time scales involved in the subsequent survival analysis, despite the relatively high magnitude of shrinkage for certain parameters due to non-uniform information provided by the retrospective data.

Thorough investigations among the potential prognostic factors identified during exploratory survival analysis have been conducted. Certain baseline variables already served as submodel covariates, such as resected tumor volume, resect organ number, surgical blood loss, and tumor multifocality, so they indirectly influenced hazards in the current results instead of being predictors in the TTE models.[10–12] We also tested whether there was a substitute for each longitudinal biomarker as a time-specific predictor of survival duration, because the established population submodels enabled prediction at arbitrary time point.[42] It only worked out for TP on day 7 which exhibited monotonicity versus time, whereas continuous BMI and WBCs, where diverse postoperative patterns have been observed in the population, must remain in the TTE models. The predictors in the final link functions outperformed other longitudinal model-derived metrics, such as daily biomarker predictions, extremum, or duration of TP/WBC abnormality, etc. Clinical reference ranges were considered during model construction, including 60 g/L as the lower limit of serum TP and 10×10^9 cells/L as the upper limit of the WBC count. Metrics related to tumor relapse also significantly correlated with OS based on univariate Kaplan–Meier analysis as reported in literature.[13,43] Nevertheless, inclusion of tumor relapse in the OS model resulted in insignificant improvement so it was excluded from the final model. The long computational times of the BMI and WBC submodels did not allow for simultaneous estimation when linking the longitudinal submodel predictions to the TTE models. Therefore, a sequential modeling strategy was adopted, using EBE-derived predictions from the submodels as predictors of survival.[15] The evaluation results suggested that the TTE models reasonably predicted OS and PFS along with the effects of key covariates on hazards in our cohort.

The study has some limitations. The predictive performance of the models has not been tested by external validation, and the high proportions of right censoring observed in this retrospective database (57.5% for OS and 36.2% for PFS) are partially determined by the disease pathology and random patient inclusion. As for the extreme censoring data where the individual event-free survival was longer than the maximum observed event time, winsorization was performed to enhance model stability.[44,45] Given the low disease prevalence, new data are consistently collected to establish a validation dataset and update follow-up

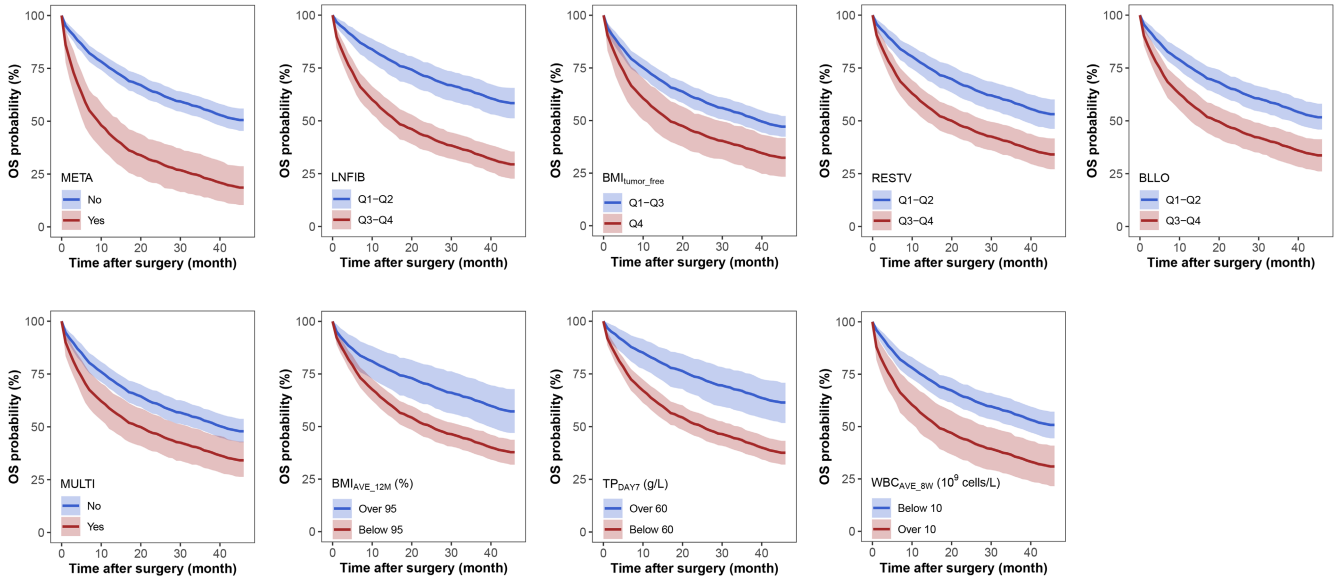

FIGURE 4 Simulated Kaplan–Meier curves of OS stratified by critical variables. Solid lines and shaded areas represent the mean and 95% confidence interval of simulated Kaplan–Meier curves of OS based on 500-cohort simulations. BLLO, surgical blood loss; BMI_{AVE_12M}, 12-month cumulative average of percentage body mass index predictions; $BMI_{tumor-free}$, tumor-free BMI; LNFIB, logarithm of fibrinogen; META, baseline metastasis; MULTI, multifocality; OS, overall survival; RESTV, resected tumor volume; TP_{DAY7}, total protein level prediction on day 7; WBC_{AVE_8W}, 8-week cumulative average of white blood cell count predictions. Q1–Q4 represents the first to the fourth quartile.

information, in order to verify the established models and to assess the survival benefits from normalized BMI/TP/WBC following intervention. Moreover, because access to the current quantitative methodology is restricted to only modelers, a user-friendly interactive website for physicians will be developed in future studies to facilitate clinical application.

In summary, the current work identified longitudinal BMI, TP, and WBC with prognostic significance in postoperative patients with RPS utilizing quantitative modeling strategies, and converted the short-term observations acquired from routine clinical surveillance into personalized prediction of long-term clinical end points. The results advocated the importance of close monitoring of perioperative changes in BMI as well as laboratory values accompanied by appropriate interventions regarding malnutrition, hypoproteinemia, and leukocytosis. The modeling framework can hopefully promote improvements in precise clinical care for patients with RPS, and may have the potential to be extrapolated to other malignancies.

AUTHOR CONTRIBUTIONS

Y.Y., Z.W., and L.Y. wrote the manuscript. C.H. and T.Z. designed the research. Z.W. and X.T. performed the research. Y.Y., L.Y., Q.Y., T.W., and Q.Y. analyzed the data.

CONFLICT OF INTEREST

The authors declared no competing interests for this work.

REFERENCES

1. NCCN. Guidelines®: Soft tissue sarcoma. Version 2.2020. *National Comprehensive Cancer Network®*; 2020.
2. Matthyssens LE, Creytens D, Ceelen WP. Retroperitoneal liposarcoma: current insights in diagnosis and treatment. *Front Surg*. 2015;2:4.
3. Swallow CJ, Strauss DC, Bonvalot S, et al. Management of primary retroperitoneal sarcoma (RPS) in the adult: an updated consensus approach from the Transatlantic Australasian RPS Working Group. *Ann Surg Oncol*. 2021;28:7873-7888.
4. Carbone F, Pizzolorusso A, Di Lorenzo G, et al. Multidisciplinary management of retroperitoneal sarcoma: diagnosis, prognostic factors and treatment. *Cancer (Basel)*. 2021;13:4016.
5. Gronchi A, Strauss DC, Miceli R, et al. Variability in patterns of recurrence after resection of primary retroperitoneal sarcoma (RPS): a report on 1007 patients from the multi-institutional collaborative RPS working group. *Ann Surg*. 2016;263:1002-1009.
6. Tan MC, Brennan MF, Kuk D, et al. Histology-based classification predicts pattern of recurrence and improves risk stratification in primary retroperitoneal sarcoma. *Ann Surg*. 2016;263:593-600.
7. Tirotta F, Parente A, Hodson J, Desai A, Almond LM, Ford SJ. Cumulative burden of postoperative complications in patients undergoing surgery for primary retroperitoneal sarcoma. *Ann Surg Oncol*. 2021;28:7939-7949.
8. Li CP, Wang Z, Liu BN, et al. Pancreaticoduodenectomy for retroperitoneal sarcomas: a mono-institutional experience in China. *Front Oncol*. 2020;10:548789.
9. Li X, Wu T, Xiao M, Wu S, Min L, Luo C. Adjuvant therapy for retroperitoneal sarcoma: a meta-analysis. *Radiat Oncol*. 2021;16:196.

10. Xue G, Wang Z, Li C, et al. A novel nomogram for predicting local recurrence-free survival after surgical resection for retroperitoneal liposarcoma from a Chinese tertiary cancer center. *Int J Clin Oncol*. 2021;26:145-153.
11. Gronchi A, Miceli R, Shurell E, et al. Outcome prediction in primary resected retroperitoneal soft tissue sarcoma: histology-specific overall survival and disease-free survival nomograms built on major sarcoma center data sets. *J Clin Oncol*. 2013;31:1649-1655.
12. Raut CP, Callegaro D, Miceli R, et al. Predicting survival in patients undergoing resection for locally recurrent retroperitoneal sarcoma: a study and novel nomogram from TARPSWG. *Clin Cancer Res*. 2019;25:2664-2671.
13. Callegaro D, Barretta F, Swallow CJ, et al. Longitudinal prognostication in retroperitoneal sarcoma survivors: development and external validation of two dynamic nomograms. *Eur J Cancer*. 2021;157:291-300.
14. Zheng Y, Narwal R, Jin C, et al. Population modeling of tumor kinetics and overall survival to identify prognostic and predictive biomarkers of efficacy for durvalumab in patients with urothelial carcinoma. *Clin Pharmacol Ther*. 2018;103:643-652.
15. Krishnan SM, Laarif SS, Bender BC, Quartino AL, Friberg LE. Tumor growth inhibition modeling of individual lesion dynamics and interorgan variability in HER2-negative breast cancer patients treated with docetaxel. *CPT Pharmacometrics Syst Pharmacol*. 2021;10:511-521.
16. Diekstra MH, Fritsch A, Kanefendt F, et al. Population modeling integrating pharmacokinetics, pharmacodynamics, pharmacogenetics, and clinical outcome in patients with sunitinib-treated cancer. *CPT Pharmacometrics Syst Pharmacol*. 2017;6:604-613.
17. Irurzun-Arana I, Asin-Prieto E, Martin-Algarra S, Troconiz IF. Predicting circulating biomarker response and its impact on the survival of advanced melanoma patients treated with adjuvant therapy. *Sci Rep*. 2020;10:7478.
18. Terranova N, French J, Dai H, et al. Pharmacometric modeling and machine learning analyses of prognostic and predictive factors in the JAVELIN Gastric 100 phase III trial of avelumab. *CPT Pharmacometrics Syst Pharmacol*. 2022;11:333-347.
19. Desmee S, Mentre F, Veyrat-Follet C, Sebastien B, Guedj J. Using the SAEM algorithm for mechanistic joint models characterizing the relationship between nonlinear PSA kinetics and survival in prostate cancer patients. *Biometrics*. 2017;73:305-312.
20. Bender BC, Schindler E, Friberg LE. Population pharmacokinetic-pharmacodynamic modelling in oncology: a tool for predicting clinical response. *Br J Clin Pharmacol*. 2015;79:56-71.
21. Al-Huniti N, Feng Y, Yu JJ, et al. Tumor growth dynamic modeling in oncology drug development and regulatory approval: past, present, and future opportunities. *CPT Pharmacometrics Syst Pharmacol*. 2020;9:419-427.
22. Venkatakrishnan K, van der Graaf PH. Model-informed drug development: connecting the dots with a totality of evidence mindset to advance therapeutics. *Clin Pharmacol Ther*. 2021;110:1147-1154.
23. Zhudenkov K, Gavrilov S, Sofronova A, et al. A workflow for the joint modeling of longitudinal and event data in the development of therapeutics: tools, statistical methods, and diagnostics. *CPT Pharmacometrics Syst Pharmacol*. 2022;11:425-437.
24. Mould DR, Upton RN. Basic concepts in population modeling, simulation, and model-based drug development. *CPT Pharmacometrics Syst Pharmacol*. 2012;1:e6.
25. Holford N. A time to event tutorial for pharmacometricians. *CPT Pharmacometrics Syst Pharmacol*. 2013;2:e43.
26. Chen W, Li L, Ji S, Song X, Lu W, Zhou T. Longitudinal model-based meta-analysis for survival probabilities in patients with castration-resistant prostate cancer. *Eur J Clin Pharmacol*. 2020;76:589-601.
27. Dayneka NL, Garg V, Jusko WJ. Comparison of four basic models of indirect pharmacodynamic responses. *J Pharmacokinet Biopharm*. 1993;21:457-478.
28. Laird AK. Dynamics of tumor growth. *Br J Cancer*. 1964;13:490-502.
29. Friberg LE, Henningsson A, Maas H, Nguyen L, Karlsson MO. Model of chemotherapy-induced myelosuppression with parameter consistency across drugs. *J Clin Oncol*. 2002;20:4713-4721.
30. Xie F, Van Bocxlaer J, Colin P, et al. PKPD modeling and dosing considerations in advanced ovarian cancer patients treated with cisplatin-based intraoperative intraperitoneal chemotherapy. *AAPS J*. 2020;22:96.
31. Thai HT, Mentre F, Holford NH, Veyrat-Follet C, Comets E. Evaluation of bootstrap methods for estimating uncertainty of parameters in nonlinear mixed-effects models: a simulation study in population pharmacokinetics. *J Pharmacokinet Pharmacodyn*. 2014;41:15-33.
32. Stillwell AP, Ho YH, Veitch C. Systematic review of prognostic factors related to overall survival in patients with stage IV colorectal cancer and unresectable metastases. *World J Surg*. 2011;35:684-692.
33. Hauser CA, Stockler MR, Tattersall MH. Prognostic factors in patients with recently diagnosed incurable cancer: a systematic review. *Support Care Cancer*. 2006;14:999-1011.
34. Lu Z, Yang L, Yu J, et al. Change of body weight and macrophage inhibitory cytokine-1 during chemotherapy in advanced gastric cancer: what is their clinical significance? *PLoS One*. 2014;9:e88553.
35. Dalal S, Hui D, Bidaut L, et al. Relationships among body mass index, longitudinal body composition alterations, and survival in patients with locally advanced pancreatic cancer receiving chemoradiation: a pilot study. *J Pain Symptom Manag*. 2012;44:181-191.
36. Kubota T, Hiki N, Sano T, et al. Prognostic significance of complications after curative surgery for gastric cancer. *Ann Surg Oncol*. 2014;21:891-898.
37. Benej M, Capov I, Skrickova J, et al. Association of the postoperative white blood cells (WBC) count in peripheral blood after radical surgical treatment of left upper lobe non-small cell lung cancer (NSCLC) with overall survival – single center results. *Bratisl Lek Listy*. 2017;118:299-301.
38. Chowell D, Yoo SK, Valero C, et al. Improved prediction of immune checkpoint blockade efficacy across multiple cancer types. *Nat Biotechnol*. 2021;40:499-506.
39. Watanabe T, Kinoshita T, Itoh K, et al. Pretreatment total serum protein is a significant prognostic factor for the outcome of patients with peripheral T/natural killer-cell lymphomas. *Leuk Lymphoma*. 2010;51:813-821.
40. Jacqmin P, Snoeck E, van Schaick EA, et al. Modelling response time profiles in the absence of drug concentrations: definition and performance evaluation of the K-PD model. *J Pharmacokinet Pharmacodyn*. 2007;34:57-85.
41. Evans ND, Cheung SYA, Yates JWT. Structural identifiability for mathematical pharmacology: models of myelosuppression. *J Pharmacokinet Pharmacodyn*. 2018;45:79-90.

42. Feng Y, Wang X, Suryawanshi S, Bello A, Roy A. Linking tumor growth dynamics to survival in ipilimumab-treated patients with advanced melanoma using mixture tumor growth dynamic modeling. *CPT Pharmacometrics Syst Pharmacol*. 2019;8:825-834.
43. Tardivon C, Desmee S, Kerioui M, et al. Association between tumor size kinetics and survival in patients with urothelial carcinoma treated with atezolizumab: implication for patient follow-up. *Clin Pharmacol Ther*. 2019;106:810-820.
44. Bietenbeck A, Cervinski MA, Katayev A, Loh TP, van Rossum HH, Badrick T. Understanding patient-based real-time quality control using simulation modeling. *Clin Chem*. 2020;66:1072-1083.
45. Wilcox RR. *Introduction to Robust Estimation and Hypothesis Testing*. 3rd ed. Elsevier; 2012.

SUPPORTING INFORMATION

Additional supporting information can be found online in the Supporting Information section at the end of this article.

How to cite this article: Yao Y, Wang Z, Yong L, et al. Longitudinal and time-to-event modeling for prognostic implications of radical surgery in retroperitoneal sarcoma. *CPT Pharmacometrics Syst Pharmacol*. 2022;11:1170-1182. doi:10.1002/psp4.12835